Metal–Organic Frameworks for Regeneration of Degraded Liquid Crystals

Wei Lee[abc], Cheng-Ting Huang[b], Kun-Ting Liao[b], Jy-Shan Hsu[bc] & Chia-Her Lin[cd]

[a] Institute of Imaging and Biomedical Photonics, National Chiao Tung University, Tainan, Taiwan

[b] Department of Physics, Chung Yuan Christian University, Chungli, Taiwan

[c] Center for Nanotechnology, Chung Yuan Christian University, Chungli, Taiwan

[d] Department of Chemistry, Chung Yuan Christian University, Chungli, Taiwan
Published online: 06 Dec 2014.

PLEASE SCROLL DOWN FOR ARTICLE

Taylor & Francis
Taylor & Francis Group

Metal–Organic Frameworks for Regeneration of Degraded Liquid Crystals

WEI LEE,[1,2,3,*] CHENG-TING HUANG,[2] KUN-TING LIAO,[2]
JY-SHAN HSU,[2,3] AND CHIA-HER LIN[3,4]

[1]Institute of Imaging and Biomedical Photonics, National Chiao Tung
University, Tainan, Taiwan
[2]Department of Physics, Chung Yuan Christian University, Chungli, Taiwan
[3]Center for Nanotechnology, Chung Yuan Christian University, Chungli, Taiwan
[4]Department of Chemistry, Chung Yuan Christian University, Chungli, Taiwan

This paper is concerned with the dramatic purification effect of porous metal–organic frameworks (MOFs) and regeneration of a degraded liquid crystal (LC) as leftover from a flat-panel production line. By soaking MOFs in the LC, the correlation between the recovery of electrical properties and the water-sorption capacity of MOFs is unambiguously revealed. Experimental evidence from the data of voltage-dependent capacitance, dielectric spectroscopy and voltage holding ratio strongly suggests that the primary contaminant in a LC leftover is moisture. This investigation paves the way for feasible recycling of deteriorated LC materials. The approach reported in this study can be applied to many fluids for purification and regeneration.

Keywords Liquid crystals; metal-organic frameworks; impurity ions; dielectric spectroscopy; voltage holding ratio; recycling

Introduction

Metal–organic frameworks (MOFs) are a new class of hybrid inorganic–organic compounds as microporous and mesoporous materials that significantly outperform many established materials such as activated carbons and zeolites in terms of the adsorption capacity [1, 2]. With suitable building blocks, the modular-construction principle of MOFs permits a rational design of these custom-made porous systems for a wide spectrum of applications including storage, sensing, transformation, or separation of atomic and molecular species inside MOFs. Taking advantage from their high adsorption capacity, one may expect the potential employment of MOFs as an effective impurity remover to regenerate liquid-crystal (LC) materials which are left over from the panel production line and somehow unavoidably contaminated when the containers are opened during the cell filling process.

Recently, we have demonstrated that natural deterioration of LCs stored under normal conditions can be primarily attributable to ion contamination caused by permeation of water

---

Color versions of one or more of the figures in the article can be found online at www.tandfonline.com/gmcl.

vapor from air into the materials [3]. Using a novel complex magnesium coordination polymer M2B, [Mg$_2$(BTEC)], where BTEC stands for 1,2,4,5-bezenetetracarboxylate anion) with remarkably desiccative capacity [4], we have further illustrated that a good level of electrically resistive quality comparable to that of a fresh LC counterpart can be recovered from a degraded sample via chemical adsorption [3]. By extending our efforts at novel materials for recuperating the electrically resistive properties of contaminated LCs, this study focuses on the effect of various novel MOFs as functional materials on recovering (i.e., levitating) the electrical resistivity of ion-contaminated LC leftovers from the panel production line of a local display manufacturer. With direct experimental evidence obtained from the voltage-dependent capacitance measurements, low-frequency impedance spectroscopy and the voltage holding ratio, the great potential of MOFs as effective purifiers for regeneration of LCs is manifest by their drastic reduction in content of impurity ions in a LC leftover. Because the current worldwide LC-display (LCD) market exceeds \$100B, the strategy revealed in this work can be promising not only in dramatically reducing key materials and manufacturing costs but also in preserving the environment for future generations.

Materials and Methods

LC Materials

The LC materials, including pristine and leftover samples used in this study, were obtained from Wintek Corporation, a Taiwan-based company and manufacturer of touch-panel and small-to-medium-sized LCDs. Here we designate the neat material GN, the leftover GL, and GL treated (i.e., purified) by a MOF material as GL-P. According to the datasheet supplied by the vender, the clearing point of GN was ∼100°C, the resistivity was ∼10^{13} Ω·cm and the moisture content ≤ 200 ppm. Note that GN is currently employed in commercialized thin-film-transistor (TFT)–LCD products.

MOF Materials and Their Properties

A series of MOFs were fabricated with metal oxygen central cage clusters interconnected by multifunctional organic linkers, yielding three-dimensional (3D) porous networks with high inner surface areas and large pore volumes. The only microporous framework synthesized in this study is known as HKUST-1 with the formula [Cu$_3$(btc)$_2$(H$_2$O)$_3$] and a pore size about 10 Å [5]. Additionally, three mesoporous frameworks—MIL-100(Al), MIL-100(Cr) and MIL-101(Cr)—were studied. They have the following formulas: [M$_3$F(H$_2$O)$_2$O(btc)$_2$]·nH$_2$O (M = Al, Cr; n 24 to 28.5; btc = benzene-1,3,5-tricarboxylate anion) with porosity originating from both 25 and 29 Å mesopores (designated MIL-100(Al) and MIL-100(Cr), respectively) [6], and [Cr$_3$(O)(bdc)$_3$(F)(H$_2$O)$_2$]·nH$_2$O (n ∼ 25; bdc = benzene-1,4-dicarboxylate anion) with pore sizes up to 34 Å (designated MIL-101(Cr)) [7]. In comparison with hydrophilic MOFs like HKUST-1, the decomposition of these mesoporous frameworks is not an issue. Table 1 presents some comparative characteristics of the investigated MOFs.

In order to make a sorption kinetic comparison, all ∼1 g sorbents contained separately in Petri dishes were preheated at 150°C for 12 h in a vacuum oven then cooled down to room temperature. The samples were then set under the experimental conditions where the temperature and relative humidity were carefully controlled at 26 ± 1°C and 50 ± 5%, respectively. The time-evolved weight gains by atmospheric water adsorption were measured.Figure 1 shows selectively the water-sorption kinetics of three vacuum-dried

Table 1. Comparative characteristics of the investigated MOFs

MOFs materials	Chemical composition	Surface area (m^2g^{-1})	Pore size (Å)	Moisture sensitivity	Color
MIL-101(Cr)	$[Cr_3(O)(bdc)_3(F)(H_2O)_2]\cdot$ $\sim25H_2O$	2800–4230	29, 34	stable	green
MIL-100(Cr)	$[Cr_3F(H_2O)_2O(btc)_2]\cdot$ $\sim28H_2O$	~2000	25, 29	stable	green
MIL-100(Al)	$[Al_3F(H_2O)_2O(btc)_2]\cdot$ $\sim24H_2O$	~2150	25, 29	stable	colorless
HKUST-1	$[Cu_3(btc)_2(H_2O)_3]$	1500–2000	10	stable	blue

mesoporous MOF samples compared with that of commercial silica gels (SiO_2). It is obvious from the figure that their extraordinarily high water-absorption capability surpasses that of silica gels, suggesting that MOFs as superior water adsorbents can be used for purification of contaminated LCs. Table 2 displays comparatively the saturated water adsorption capacities and saturation times of various sorbents including M2B, SiO_2 and HKUST-1. One can see how the mesoporous MOFs outperform the other counterparts.

Cell Fabrication

MOFs as LC purifiers were pretreated by baking in a vacuum oven at 150 °C for 12 h to ensure their dryness. Each dried purifier in a specific amount was put in a vial containing GL for an appropriate period of time. The treated LC in each vial having MOF sediment at the bottom was then introduced by capillary action into an empty cell at 120°C (i.e., in the isotropic state) with a syringe with a disc membrane filter. Each empty cell with an air gap of 6.7 ± 0.1 μm was constructed with a pair of electrically conducting glass substrates coated with polyimide alignment layers for antiparallel configuration. The structure and geometry of the cell can be found elsewhere [8]. The LC cells were used in various experiments to
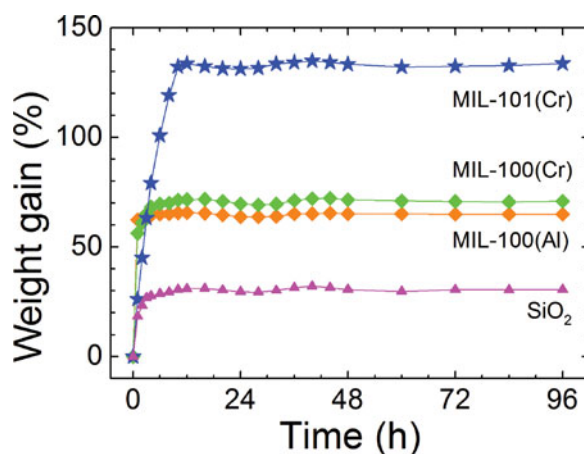

Figure 1. Time-evolved weight gains by atmospheric water adsorption in dried mesoporous frameworks and silica gels.

Table 2. Water-absorption characteristics of various porous materials

| Sorbent	Saturated water-adsorption capacity	Saturation time (h)
MIL-101(Cr)	135%	12
MIL-100(Cr)	70%	12
MIL-100(Al)	65%	12
M2B	60%	96
SiO$_2$	30%	12
HKUST-1	25%	12

be described in the following subsection. Figure 2 illustrates the process of the LC cell fabrication.

Measurements

The voltage-dependent capacitance data were acquired with an LCR meter (Agilent E4980A). While the dc signal was supplied at ramping amplitudes from 0 to 30 V and back to 0 V and with every 0.1-V step lasting for 0.5 s, the 0.01-V$_{rms}$ probe voltage for capacitance measurement was a sinusoidal waveform at 1 kHz. The precision LCR meter was interfaced with a computer, forming a LabVIEW-controlled instrumentation.

Dielectric spectroscopy was carried out with another LCR meter (HIOKI 3522-50 LCR HiTESTER) having capability of measurement in the frequency range from 1 mHz to 100 kHz and basic measurement accuracy of $\pm 0.08\%$. The amplitude of the sinusoidal probe voltage was 0.5 V$_{rms}$. The frequencies ranged from 10^{-1}–10^5 Hz. The obtained complex (namely, real-part and imaginary-part) dielectric constants were used to calculate the conductivity and the concentration of impurity ions in a LC [9].

The voltage holding ratio is one of the most important parameters as a measure of LCD performance. The ideal value of unity (i.e., 100%) cannot be achieved in a real device. For all active-matrix-driving LCDs, the ratio must be high enough to ensure their device performance. We measured the voltage-holding-ratio values of various cell samples of GN, GL and GL-P by means of our homemade instrument. This LabVIEW-controlled instrument, designed for the fully integrated solution for automated high-precision measurements of
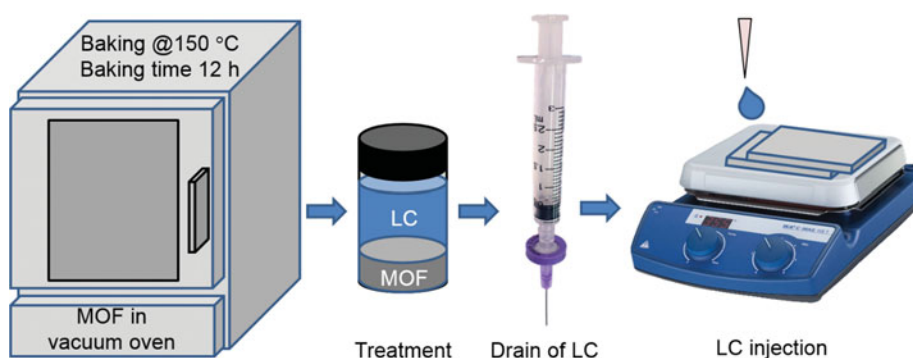
Figure 2. Process of the preparation of LC cells for measurements.

the voltage-holding-ratio and residual-direct-current properties [10], features its small size (270 × 180 × 140 mm), low weight (4.5 kg), high portability, ease of operation and low cost. In this study, the experimental conditions (data-line and scan-line signals *etc.*) and the formula for calculating the voltage holding ratio followed what has been reported in a previous work [11].

Dielectric spectroscopy and measurements of voltage-dependent capacitance as well as the voltage holding ratio were employed to analyze the ability of distinct MOF materials in recuperation of the desired device performance of a degraded industrial LC. All the data were compared between regenerated LCs and their fresh counterpart.

Results and Discussion

Based on the data presented in Table 2, here we focus on our findings concerning the effects of MIL-101(Cr) and MIL-100(Cr) against HKUST-1. For simplicity, a GL sample purified by MIL-101(Cr) is termed GL-P1. Likewise, GL purified with MIL-100(Cr) and HKUST-1 are designated GL-P2 and GL-P3, respectively.

The voltage-dependent-capacitance data for each LC cell yielded a loop in the voltage–capacitance (V–C) plot. In the voltage ramping-up process, one can define a voltage parameter V_{up} where a 10% increase in capacitance is found. Similarly on the ramping-down curve, one can obtain a higher voltage V_{down} corresponding to the same capacitance. The two curves are not overlapped ideally because of the accumulation of ions on the electrodes in a static electric field [12]. Figure 3 depicts a typical V–C plot, which was obtained from a GL cell. Experimental demonstration of the effect of MOFs on the improved electrical property has been reported elsewhere [13]. Note that the V–C loop exhibits a certain width at the arithmetic average of the minimum and maximum values of capacitance. This conventionally defines the hysteresis width H. In Table 3, several voltage parameters, including the threshold-voltage difference ΔV_{th} between V_{down} and V_{up}, are displayed for five samples including GL-P treated with MIL-101(Cr), MIL-100(Cr) and HKUST-1 at MOF concentration of 1 wt% for soaking time of 24 h. It is clear from the table that the effects of the MOFs on purification of contaminated LC were obvious. Moreover, the best result was obtained from GL-P1, indicating that MIL-101(Cr) served as the most
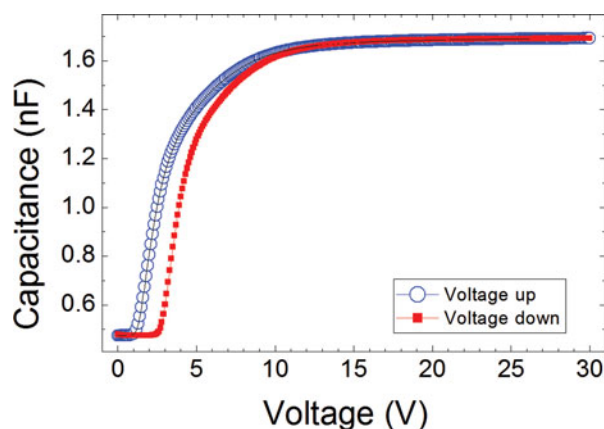

Figure 3. Capacitance as a function of dc voltage of a GL (leftover-LC) cell.

Table 3. Voltage properties of various LC samples deduced from *V–C* curves

Sample	V_{up} (V)	V_{down} (V)	ΔV_{th} (V)	H (V)
GN	1.30	1.50	0.20	0.10
GL-P1	1.30	1.55	0.25	0.30
GL-P2	1.35	2.20	0.85	0.80
GL-P3	1.40	2.70	1.30	1.10
GL	1.50	3.00	1.50	1.40

effective ion-remover among all porous materials studied, which is in good agreement with Figure 1 and Table 2. The correlation between the ion-removal effect and water adsorption capacity is easily understood in that water molecules embedded in a LC, if any, can form both H^+ and OH^- ions, generating an enormous amount of impurity ions to demote the LC device performance under an applied voltage.

The dielectric data, including the real-part dielectric function and the imaginary-part dielectric function, allowed one to deduce the ion concentration and diffusion constant [14]. For a comparative experiment involving soaking distinct amounts (0.1, 0.5 and 1.0 wt%) of MOFs separately in GL for 24 h to remove impurity ions, the calculated charge densities and the resulting ion-removal ratios are listed in Table 4. Rationally, the charge density decreased with increasing MOF concentration for a given treatment time. It is worth mentioning that the ion-removal ratio, defined as the ratio of the difference between the ion concentration in GL and that in GL-P to the ion concentration in GL, was quite high for degraded LC treated with any MOF material at 1.0 wt%. In this condition, the effects of the three MOFs were almost identical in terms of reducing mobile ions. The results displayed in Table 4 indicate that the concentration of impurity ions found in a leftover TFT-grade LC can dramatically be reduced by treatment (i.e., soaking) with the MOF materials.

Table 4. Charge densities and the corresponding ion-removal ratios of various samples

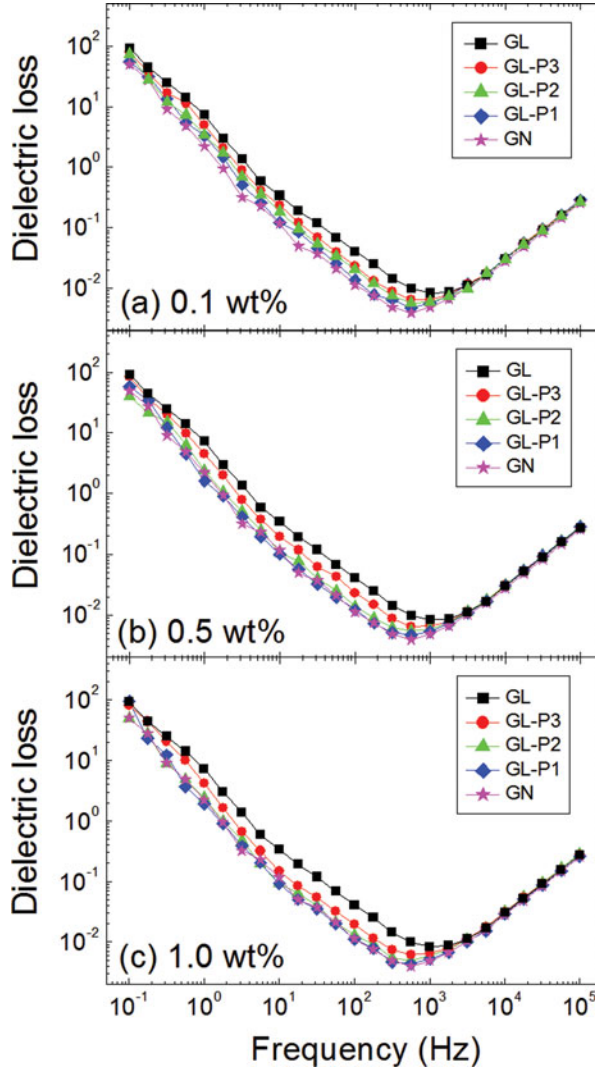| MOF concentration	Sample	Charge density (nC/cm^3)	Ion-removal ratio (%)
	GN	0.092	
	GL	0.108	
0.1 wt%	GL-P1	0.111	89.7
	GL-P2	0.178	88.5
	GL-P3	0.156	85.6
0.5 wt%	GL-P1	0.194	98.2
	GL-P2	0.310	97.1
	GL-P3	0.525	95.1
1.0 wt%	GL-P1	0.162	98.5
	GL-P2	0.214	98.0
	GL-P3	0.306	97.2

Figure 4. Frequency-dependent dielectric loss of untreated LC samples GL (leftover) and GN (neat) and GL-P (purified) treated with MOFs at (a) 0.1 (b) 0.5 and (c) 1.0 wt% for 24 h.

Figure 4 delineates the dielectric loss function $\varepsilon''(f)$ of various LC samples. Note that the ac conductivity is determined by $\varepsilon''(f)$ with the following relation:

$$\sigma_{ac} = 2\pi f \varepsilon_0 \varepsilon''(f), \tag{1}$$

where f denotes the frequency and ε_0 stands for the permittivity in free space. The dc term can thus be calculated by curve fitting using the formula [3]

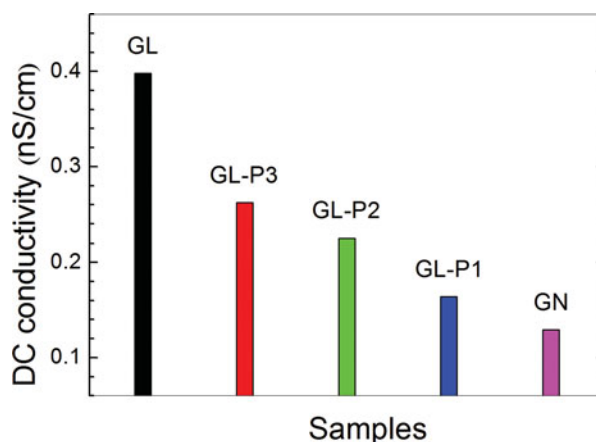$$\sigma_{dc} = \sigma_{ac} - sf^m, \tag{2}$$

Figure 5. DC conductivities of untreated GL (leftover) and GN (neat) samples as well as GL-P treated with MOFs at 1.0 wt% for 24 h. The data are deduced from Figure 4(c).

where σ_{dc} represents the dc conductivity, which is independent of frequency. The results for GL-P samples treated individually with 1.0-wt% MOFs are shown in Figure 5. Referring to Table 4, one can see that σ_{dc} increased with increasing charge density. However, the proportionality cannot completely be held because the dc conductivity is actually proportional to the multiplication of the ionic concentration and the diffusion constant [15].

Figure 6 shows the comparison between the water-sorption kinetics of MIL-101(Cr) and the voltage holding ratio of a GL-P1 cell varying with the treatment time, where the concentration of MIL-101(Cr) was 1.0 wt%. Note that the inset of Figure 6 is retrieved from Figure 1 and Figure 6 reveals the voltage holding ratio of GL-P as a function of the MOF treatment time. Clearly, the time-evolved voltage holding ratio curve resembles the kinetic weight gain although the time scales are not the same. The significance of such observation is that the primary source of impurity ions in the leftover LC was, indeed, water molecules trapped in the LC material. This finding indicates that MOFs are applicable to the
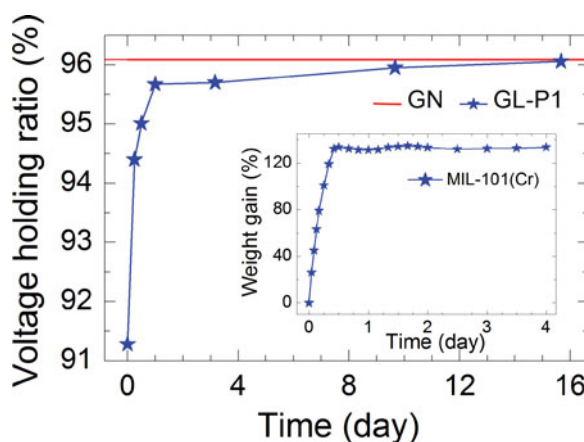

Figure 6. Voltage holding ratio of GL-P1 (leftover treated with MIL-101(Cr)) as a function of treatment time resembling the curve of water-sorption kinetics of MIL-101(Cr).

purification and, in turn, capable of recovering the electrical and electro-optical properties of LCs through their intrinsic moisture-absorption characteristics [13].

Conclusions

We disclose in this paper that the primary contaminant in liquid crystal leftovers, retrieved from flat-panel production lines, originate actually from moisture in the air instead of artificial contamination. Experiments involving the voltage-dependent capacitance measurement, low-frequency impedance spectroscopy and the voltage-holding-ratio measurement were performed in order to compare the electrical and ionic properties between a leftover (i.e., degraded) sample and its brand-new (i.e., fresh) counterpart. Supplied with strong experimental evidence, we unambiguously demonstrate, for the first time to our best knowledge, the great potential of metal–organic frameworks as effective purifiers for regeneration of the liquid crystal because of the dramatically reduced concentration of impurity ions in the leftover. By soaking porous metal–organic frameworks in deteriorated liquid crystals, this approach is proved to be very simple and cost-effective, allowing sustainable management and conservation of resources for the current $100B liquid-crystal-display market, thereby preserving the environment.

Acknowledgments

Funding

References

[1] Devic, T., & Serre, C. (2009). In: *Ordered Porous Solids*, Elsevier: New York, Ch. 4, pp. 77–99.
[2] Zhou, H.-C., Long, J. R., & Yaghai, O. M. (2012). *Chem. Rev.*, *112*, 673.
[3] Lee, W., Wang, C.-T., & Lin, C.-H. (2010). *Displays*, *31*, 160.
[4] Liu, H.-K., Tsao, T.-H., Lin, C.-H., & Zima, V. (2010). *Cryst. Eng. Comm.*, *12*, 1044.
[5] Chui, S. S.-Y., Lo, S. M.-F., Charmant, J. P. H., Orepn, A. G., & Williams, I. D. (1999). *Science*, *283*, 1148.
[6] Férey, G., Serre, C., Mellot-Draznieks, C., Millange, F., Surblé, S., Dutour, J., & Margiolaki, I. (2004). *Angew. Chem.*, *116*, 6456.
[7] Férey, G., Mellot-Draznieks, C., Serre, C., Millange, F., Dutour, J., Surblé, S., & Margiolaki, I. (2005). *Science*, *309*, 2040.
[8] Lee, W., & Chen, H.-C. (2003). *Nanotechnology*, *14*, 987.
[9] Jian, B.-R., Tang, C.-Y., & Lee, W. (2011). *Carbon*, *49*, 910.
[10] Lin, Y.-T., & Lee, W. Taiwan Patent No. I 379094, issued 12/11/2012.
[11] Tang, C.-Y., Huang, S.-M., & Lee, W. (2011). *J. Phys. D: Appl. Phys.*, *44*, 355102.
[12] Lee, W., Wang, C.-Y., & Shih, Y.-C. (2004). *Appl. Phys. Lett.*, *85*, 513.
[13] Huang, C.-T., Liao, K.-T., Hsu, J.-S., Lin, C.-H., & Lee, W. (2013). *Appl. Phys. Express*, *6*, 121701.
[14] Liu, H.-H., & Lee, W. (2010). *Appl. Phys. Lett.*, *97*, 023510.
[15] Lin, F.-C., Wu, P.-C., Jian, B.-R., & Lee, W. (2013). *Adv. Cond. Mat. Phys.*, *2013*, 271574.